Research Article

Optimization of a Dry Peeling System for Tomatoes Using Approximate Solutions

*A. Metallo ⓘD

Industrial Engineering Department, University of Salerno, Italy
E-mail: antonio. metallo@libero.it

Abstract

In recent years tomatoes have been peeled using steam and lye. Both are costlier, less environmentally friendly and highly polluting techniques. Thus, more sustainable alternatives should be sought after. Among these alternatives is radiative heating. To appropriately design the system for dry peeling, several typical operational characteristics of the process in issue must be estimated. The analytical model presented allows estimates to be made through closed-form relationships between the parameters involved. The analysis is based on the use of an appropriate theoretical model, which facilitates the solution to the proposed problems. Through the approximate solution of the analytical problem, we will analyse: the angular speed Ω, the temperature fluctuations ΔT_0, the process time t_c. These estimates are then used to derive a specific model for a control of process. The temperature profile (through an approximate solution) associated with the process that provides the optimum peel quality was utilized as a guide for the regulation system. A control system used the code to extract a specific temperature, and based on surface tomato temperature readings, controlled a brushless motor using a logic strategy. The regulating system can adjust the rotation speed, and hence the heating intensity, even under less than perfect operating conditions in order to obtain the appropriate profile temperature. The controlled temperature profile yielded an average temperature of 66.3°C, while the reference case yielded a temperature of 67°C. Additionally, it was found that the temperature inaccuracy decreased with each rotation, ranging from 2.5 °C at 2π to 0.3 °C at 16π. As a result, the peeling procedure is standardized in time, temperature, and quality.

Keywords: Dry peeling system; integral method; process control, approximate solution

1. Introduction

Major issues that plague the sustainability of the tomato processing industry include energy consumption, wastewater management, and pollution [1-3]. With the development of advanced infrared dry peeling technology, the traditional hot lye method for peeling tomatoes can be replaced. This process relies on infrared heating panels to quickly heat up tomatoes, resulting in a thinner thickness of peeled-off skin and slightly firmer texture of peeled tomato. The IR dry-peeling method is rapidly adopted by food processors, due to its sustainable advantages like high efficiency and negligible water use [4, 5]. By irradiating the tomato surface with infrared radiation and selecting a suitable value of power density, temperature and time, it is possible to increase the Young's modulus of the peels. As a result, the adhesiveness of the peel is reduced. These findings demonstrated the effectiveness of the novel IR dry-peeling process for tomatoes [6]. Producing high quality peeled tomatoes is a challenging task, especially with the variety of tomato types. However, some critical aspects of peeling tomatoes using infrared radiation heating were outlined by [7]. Wishing to perform successful infrared peeling requires to realize both rapid and uniform heating on the tomato surface. An infrared heating system was designed to be installed in a food processing facility. The purpose of this research is to improve the heating uniformity of tomatoes transported along by the conveyor belt, in order to obtain an optimal design of infrared heating systems. For this purpose, the irregular shape of tomatoes and their different expositions to the heating source when transported along by the conveyor belt are to be considered. In this context, a typical configuration for industrial peeling is realized by means of a plane matrix of infrared emitters [8, 9]; looking at tomatoes in relative motion, they have been found to rotate on the belt when processed. To retrieve tomato thermal response to infrared heating, a numerical approach is necessary due to the complexity of the geometry. Previously, the authors attempted to descry the process using an analytical model: an infinite body subjected to a suitable source of pulsating heat was considered because the proper time scale was small [10, 11]. For peeling purpose, it proved useful to assume that the heating process would end a specified temperature was reached [4, 8, 12]. Achieving the best heating uniformity also means considering rotation speed and relative position to the source. To ensure uniform heating, a system for a rotation speed regulating has been proposed. After dimensioned the system and got the values of the parameters which enable to achieve the optimal temperature profile, which thus assures the proper heating uniformity and excellent quality of the product, the control logic has been established which allows us to obtain a peeling process with very comparable temperature profiles to the reference one. De facto, the

emissivity value and therefore the amount of heat transferred are influenced by factors like the size of the tomatoes, the existence of processing residues on the lamp's surface, and others [13, 14]. In order to regulate the intensity of the heat transferred, the rotation speed was adjusted.

To achieve this, the surface temperature, the logic control, and the temperature value pertaining to the reference profile must be delivered to the regulating system. A pyrometer, a mathematical model, and an approximation solution are used to supply the first, second, and third parameters, respectively. The analytic solution appears rather involved [10, 11], which affects the calculation times, thus a further approximate approach to the same problem is attempted in order to obtain an easy-to-handle solution, and therefore less run time. Since the peeling process typically takes place at a number of revolutions of n $\cong$ 10 rpm [4, 8, 12], the regulation system will have to act approximately every 6 s. The relatively long calculation times, about 2 s, moreover and the solution's complex structure make the analytical solution unusable for the proposed regulation system. While the approximate solution is obtained almost instantly. It is therefore very simple and rapid to provide the code with the function that represents the approximate solution of the problem. In this way, it is feasible to overcome the limitations noted in the literature, in which, after the ideal peeling parameters have been determined, the process always occurs under the same conditions, without taking into account the variation of thermal power transferred as the emissivity varies (different diameters , process residues on the lamp surface, etc). As a result, the method is highly dependent on the emissivity value and fails to produce a quality-standardized output. Instead, by using the dry peeling temperature control system, the peeling productivity can be significantly increased by making the process quality standardized.

2. Materials and Method

The experimental setup of Figure 8, relating to the peeling of tomatoes with radiation, belongs at the first step of Pan's activity, Li et al. [8, 12, 15, 19].
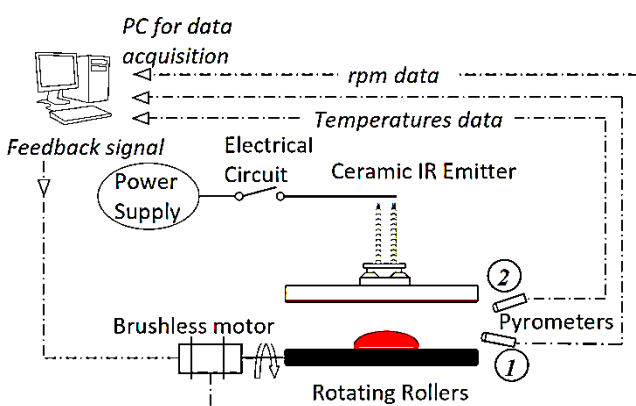

Figure 1. The experimental setup.

It consists of two main sections: IR heater, and rotating rollers. Curved ceramic emitters were adopted in the prototype equipment to enhance the IR heating intensity and the overall heating uniformity of tomatoes [8, 9, 18, 19]. Specifically created software (7.1 LabView®, National Instruments Corp., Austin, Texas) was employed for both data acquisition and reduction. The code collects the temperature data, detected by the pyrometers, for control purposes. In particular, the first pyrometer is used to obtain

the temperature of the lamp, and therefore to be able to evaluate the power transferred by it. The second supplies the surface temperature of the tomato, required for regulation system. At this point, the code extracted a specific temperature and based on such temperature reading, the computer program controlled the brushless motor, then the revolution number n, with a DAQ board (AT MIO 16XE50, National Instruments, Austin, Texas) by means of a specific logic strategy.

3. Mathematical Formulation

The theoretical study of the thermal problem involving the radiative heating of the tomato began with analytical modeling [16]. The non-linear exchange between various radiative surfaces makes heat transfer modeling in tomato IR heating difficult [21]. Several assumptions were made in the development of the heat transfer model to simplify it and reduce computational times. Such assumptions have been frequently used by researchers to develop heat transfer modeling during IR heating of food [21-24].

- Rapid processing determines only surface peripheral warming up.

- Flesh and peel materials were homogeneous, isotropic, and had similar thermal properties. For lye peeling, the surface temperature of tomatoes was assumed to be equal to the temperature of peeling solution[12].

- Constant thermal proprieties: It has been verified that the sensitivity of the temperature field to variations in properties has no effect on the thermal aspect of the problem under examination.

- Generally, tomatoes used in this study were longer in longitudinal direction (stem-blossom end) than radial direction[22]. Since the tomatoes were lined up in the longitudinal direction, the long row of tomatoes were considered as an infinitely long cylinder (i.e., the variation in the diameter of tomatoes was neglected).

- Tomato was opaque to thermal radiation (no transmission) and all incident energy was absorbed at the surface of tomato with a small reflection of incident energy (reflectivity of tomato is about 5%) [22].

- All participating radiating surfaces were diffused-grays surfaces based on the enclosure theory, which meant that each participating object could emit to and absorb radiation from each other.

- Hot air between emitter and tomato was transparent and did not interact with IR radiation passing through it. In other words, the proposed model involved heat transfer with surface to surface radiation among diffused surfaces through nonparticipating medium.

- Heat transfer within the tomato occurred only by conduction.

- Heat transfer at tomato surface occurred by radiation between emitter and tomato and convection between air and tomato. Air temperature ($T\infty$) remained constant.

- All radiation heat was incident on tomato surface only (i.e. zero penetration depth).

- Heat of generation due to respiration was neglected because it is very small compared to the total thermal energy received by tomato during IR heating.

- Mass transfer (moisture loss) was so small that the rate of heat loss due to evaporation could be neglected. Therefore, heat transfer due to evaporation (q_{evap}) during IR heating of tomatoes was assumed to be zero ($q_{evap}= 0$) [22, 26]. Thus the tomato under test is modeled as a purely conductive radiation semi-infinite body 1-D model.

The analytical approach has it purpose of estimating the process parameters and at the same time to understand the phenomenon in question. To thermally model the tomato it is necessary to carry out an evaluation of the thermophysical properties which should be close to those of water. The thermophysical properties are evaluated using the typical food constituents: water, proteins, fats, carbohydrates, fibers, and ashes. In 1986 Yonghee Choi and Martin Okos of the Purdue University in the USA, on the basis of experiments and theoretical-analytical checks [17], developed mathematical models in a range of validity between -40 and +150°C for the estimation of thermophysical properties of foods based on their composition. Table 1 shows mathematical models for estimating the following properties as function of temperature:

- thermal conductivity (k)
- thermal diffusivity (α)
- density (ρ)
- specific heat at constant pressure (c_p)

Table 1. Thermophysical Properties of Basic Nutrients; Temperature in Celsius Degrees.

Component	Models of thermophysical properties
Protein	$k=1.7881\cdot10^{-1}+1.1958\cdot10^{-3}T-2.7178\cdot10^{-6}T^2$ $\alpha=6.8714\cdot10^{-2}+4.7578\cdot10^{-4}T-1.4646\cdot10^{-6}T^2$ $\rho=1.3299\cdot10^{3}-5.1840\cdot10^{-1}T$ $c_p=2.0082+1.2089\cdot10^{-3}T-1.3129\cdot10^{-6}T^2$
Carbohydrates	$k=2.0141\cdot10^{-1}+1.3874\cdot10^{-3}T-4.3312\cdot10^{-6}T^2$ $\alpha=8.0842\cdot10^{-2}+5.3052\cdot10^{-4}T-2.3218\cdot10^{-6}T^2$ $\rho=1.5991\cdot10^{3}-3.1046\cdot10^{-1}T$ $c_p=1.5488+1.9625\cdot10^{-3}T-5.9399\cdot10^{-6}T^2$
Fats	$k=1.8071\cdot10^{-1}-2.7604\cdot10^{-3}T-1.7749\cdot10^{-7}T^2$ $\alpha=9.8777\cdot10^{-2}-1.2569\cdot10^{-4}T-3.8286\cdot10^{-8}T^2$ $\rho=9.2559\cdot10^{2}-4.1757\cdot10^{-1}T$ $c_p=1.9842+1.4733\cdot10^{-3}T-4.8008\cdot10^{-6}T^2$
Fibers	$k=1.8381\cdot10^{-1}+1.2497\cdot10^{-3}T-3.1683\cdot10^{-6}T^2$ $\alpha=7.3976\cdot10^{-2}+5.1902\cdot10^{-4}T-2.2202\cdot10^{-6}T^2$ $\rho=1.315\cdot10^{3}-3.6589\cdot10^{-1}T$ $c_p=1.8459+1.8306\cdot10^{-3}T-4.6509\cdot10^{-6}T^2$

The density of foods ρ can be calculated with the relationship:

$$\rho = (1-\zeta) / \sum(x_i/\rho_i) \tag{1}$$

where ζ is the porosity, x_i and ρ_i are respectively the mass fraction and density of the different food constituents. The specific heat of the food above the freezing temperature can be obtained from the weighted average of the specific heats of the constituent components according to the Eq. (2):

$$c_p = \sum c_i \cdot x_i \tag{2}$$

where c_i and x_i are the specific heat and the mass fraction of the different food constituents.

Several models for the estimation of k have been developed to take due account of the fibrous structure of many foods. In particular Murakami and Okos, in analogy with parallel or series connections of the electrical resistances, have proposed models that consider the anisotropy of the materials. The parallel model (p.m) is the sum of the thermal conductivities of the constituents k_i multiplied by the respective fractions in volume according to the Eq. (3):

$$k_{eq} = \sum x_{iv} \cdot k_i \tag{3}$$

The volume fraction can be obtained from the following relationship:

$$x_{iv} = (x_i/\rho_i)/\sum(x_i/\rho_i) \tag{4}$$

The mass fractions of the individual tomato constituents reported in one of the works by Pan et al the [8], were obtained from the "United States Department of Agriculture Food Composition Databases" (2010 USDA Nutrient Database) Table 2. Considering the temperature equal to 25°C and using the above equations, the thermophysical properties are calculated for each component and having determined the relative volume fractions, those of the tomato.

Table 2. Thermophysical Properties of Tomato Components and Corresponding Fractions.

Component	ρ [kg/m^3]	k [W/(mK)]	c_p [kJ/(kgK)]	x_{mass}	x_{volume}
Protein	1316.94	0.207	2.038	0.0088	0.0068
carbohydrates	1591.34	0.233	1.594	0.0389	0.0248
Fats	915.15	0.112	2.018	0.002	0.0022
Ashes	2416.78	0.363	1.138	0.005	0.0021
Water	994.91	0.611	4.171	0.9452	0.962

For tomato we obtain: $\rho = 1014.8$ kg/m^3, k = 0.596 W/(m·K) and cp = 4032 J/(kg·K). The results clearly show how strongly similar the characteristics of the tomato are to those of water.

In order to verify the validity of the parallel model, used following the assumptions made, the properties were verified to correspond to those derived from [21], obtained through the empirical formulas described by Singh and Heldman [27].

Table 3. Thermophysical properties of processing tomato with respect to temperature [21].

Thermophysical properties	Function	Temperature °C 25	Temperature °C 90	$\Delta\%$	p.m err%
Thermal Conductivity	0.0009*T[°C] +0.5495 [W/(m °C)]	0.572	0.6305	9.7	4.11
Specific Heat Capacity	0.6024*T[°C] +4020.5 [J/(kg °C)]	4035.56	4074.71	0.9	0.09
Density	0.4266*T[°C] +976.59 [kg/m3]	987.255	1014.98	2.7	2.75

As shown in the Table 3, the error incurred while utilizing the parallel approach for thermal conductivity is no more than 4%. Therefore, the applied methodology can be regarded as accurate given that the results of the sensitivity analysis demonstrate that a 10% variation in the properties corresponds to a 3.1% variation in the size itself. Consequently, the error made taking into account the constant properties is also small.

Typically, a very short warm up period of no more than 60 seconds is required for successful peeling of surfaces at

temperatures as high as 100°C [4, 8, 12, 19]. For tomato, assuming the thermo-physical properties of water apply, it can be easily demonstrated that thermal penetration depth will be limited to a few millimeters under the tomato skin, thereby permitting the semi-infinite body model to be applied [10]. Convective heat transfer also occurs at the boundary due to cycling radiative heating extended to the first half period of the sinusoidal source. Our study is concerned with a semi-infinite medium with combined third and second kind boundary conditions, incorporating both convection and periodic heating, Figure 2.
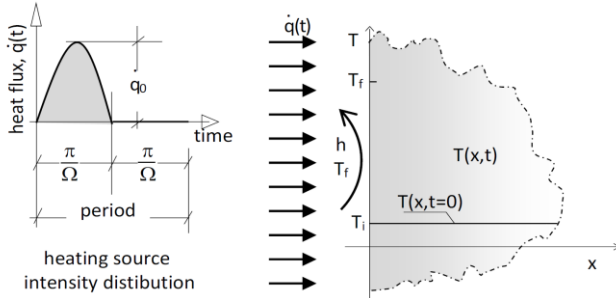

Figure 2. A schematic representation of the problem.

One-dimensional heat conduction and constant thermal properties are considered. The medium is assumed initially in equilibrium with the ambient at temperature T_0. In order to describe the heating felt by the rotating tomatoes, the surface at $x = 0$ is assumed to be exposed to a periodic on/off heat flux with ½ duty cycle; when the source is on, i.e. in the first half period, the heating intensity is assumed to vary sinusoidally with time, while it is zero in the second half, Figure 3.
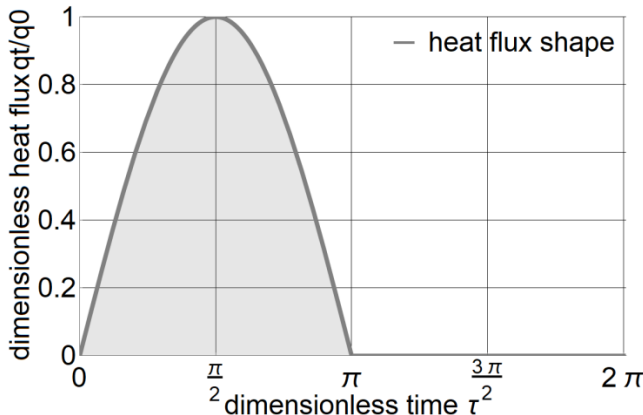

Figure 3. The dimensionless shapes for heat flux.

Therefore, periodic nonhomogeneous boundary conditions are required, which highlight the semi-amplitudes and characteristic angular speeds Ω of tomato rotation. During the peeling process, the temperature penetration depth is easily checked to ensure that it is confined to the very first layers of the tomato skin, which justifies the semi-infinite slab model [10, 11]. When constant properties are considered and heat is transferred using internal conduction, dimensionless energy balance equations and associated boundary conditions have nonhomogeneous linear properties:

$$\frac{\partial^2 \theta}{\partial \xi^2} = 2\frac{\partial \theta}{\partial \tau} \tag{5}$$

$$-\frac{\partial \theta}{\partial \xi}\bigg|_{0,\tau} = \hat{\dot{q}}(\tau) - B_i\left(\theta - \theta_f\right) \tag{6}$$

$$\theta(\xi, \tau = 0) = 0 \tag{7}$$

$$\theta(\xi \to \infty, \tau) = 0 \tag{8}$$

where the following dimensionless parameters have been introduced: $\theta = (T-T_0)/DT_{ref}$ is a dimensionless temperature, T_0 is the initial temperature; the group $DT_{ref} = \dot{q}_0 x_{ref}/k$ [K] is a reference temperature difference, $\dot{q}_0$ is the heat flux, and $x_{ref} = \sqrt{2\alpha \cdot t_{ref}}$ [m] a reference length; k [W·m^{-2}·k^{-1}] is thermal conductivity and α [m^2·s^{-1}] is the thermal diffusivity of tomato; the reference time, $t_{ref} = \Omega^{-1}$ was chosen such as the dimensionless time resulted $\tau = \Omega \cdot t$ [rad], being Ω [rad s^{-1}] the angular velocity of the source; the dimensionless space variable was defined such as $\xi = x/x_{ref}$ and, finally, $\hat{\dot{q}}(\tau) = \sin(\tau)[1+\text{sign}(\sin(\tau))]/2$ is the normalized wall heat flux, and $Bi = h x_{ref}/k$ is the Biot number.

The solution was be obtained as the sum of two partial solutions. The analytical solution of both is obtained by the application of the Laplace transform technique. The full solution (Eq. (9)), obtained and validated in the previous works [10, 11, 20] (Figure 4), turns out to be was:

$$\theta(\xi, \tau) = \theta_h(\xi, \tau) + (1+(-1)^n)\tilde{\theta}_\tau(\xi, \tau)$$
$$- 2\sum_{i=0}^{n} (-1)^i \tilde{\theta}_{i\pi}(\xi, \tau) \tag{9}$$

with

$$\tilde{\theta}_{\tilde{\tau}}(\xi, \tau) = \int \Bigg[\frac{e^{-\frac{\xi^2}{2(\tau-\tilde{\tau})}}}{\sqrt{4\pi(\tau - \tilde{\tau})}} - \frac{B_i}{2} e^{B_i\sqrt{2}\xi + B_i^2(\tau-\tilde{\tau})}$$
$$\times \text{erfc}\left(\frac{\xi}{\sqrt{2(\tau - \tilde{\tau})}} + B_i\sqrt{(\tau - \tilde{\tau})}\right)\Bigg]\sin(\tilde{\tau})d\tilde{\tau} \tag{10}$$

The term

$$\theta_h(\xi, \tau) = \theta_f\left(\text{erfc}\left(\frac{\xi}{\sqrt{2\tau}}\right) - e^{B_i\sqrt{2}\xi + \tau B_i^2}\right.$$
$$\left.\times \text{erfc}\left(\frac{\xi}{\sqrt{2\tau}} + B_i\sqrt{\tau}\right)\right) \tag{11}$$

represents the thermal response due to the convective heat transfer driven by the initial temperature excess $\theta_f = (T_0 - T_f)/DT_{ref}$, relatively to ambient temperature T_f, n is intervals of amplitude π over which $\hat{\dot{q}}(\tau)$ remains continuous and $\tilde{\tau}$ is the dummy variable of convolution.

The term $\tilde{\theta}_\tau$ is obtained from the particularization of Eq. (10) at process time.

As expected, the solution depends not only on the values at time τ, but it also depends on the heating previously experienced at each revolution ($\tilde{\theta}_{i\pi}$), i.e. at each $\tilde{\tau} = i\pi$. The temperature field is unsteady due to the spatial and temporal

coordinates and the Biot number. The oscillating trend of the temperature profiles is represented in the Figure 3 in correspondence with the surface ($\xi=0$) for different values of the Biot number. The Figure clearly shows that different entities of cooling have different thermal responses. The greater the Biot number, the more both temperature levels and the amplitude of the oscillations decrease ($\Delta\theta$,Bi=0 =0.80, $\Delta\theta$,Bi=0.5 =0.53). Can be further observed that the phase shift with respect to the heat flux decreases with Bi number (φ,Bi=0 =0.72, φ,Bi=0.5 =0.46) [11]. The analytical solution was used to validate the approximate solution.
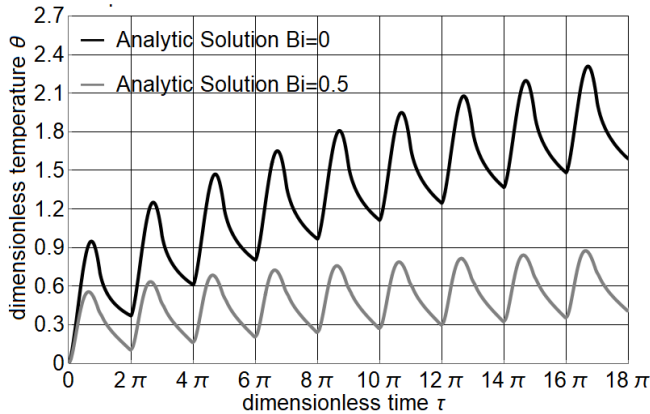

Figure 4. The dimensionless surface temperature at $\xi = 0$.

3.1 Approximate Solution

The solution obtained in the previous paragraph appears to be rather involved, so an approximate approach to the same problem is taken to achieve an easier solution. The problem was solved by applying the integral method. It was possible to obtain the solution of problem (Eqs. (5)-(8)) by choosing an approximate solution that makes explicit the dependence of the spatial variable:

$$
\begin{aligned}
\theta^*(\xi,\tau) &= a(\xi)\,\mathrm{erfi}\left(\tau^{1.5}\right) \\
&+ \left(0.443+0.255 B_i\right)\sin\left(0.5\times\tau\right)^2 \\
&+ \left(0.230-0.352 B_i\right)\sqrt{\tau} \\
&+ \left(0.186-0.156 B_i\right)\sin\left(2.112-\tau\right)^3 \\
&- \left(0.235-0.157 B_i\right)\sin\left(-\tau\right)^3 \\
&+ \left(0.158-0.181 B_i\right)\sin\left(-1.587-\tau\right) \\
&+ \left(0.207-0.101 B_i\right)\sin\left(0.418-\tau-0.512 B_i\right)^2 \\
&+ \left(0.1775-0.2483 B_i\right)\mathrm{erf}\left(-\tau\right)\left(1-1.167 B_i\right)
\end{aligned}
\tag{12}
$$

with a(ξ) unknown function which is obtained as follows. Eq. (5) has been integrated into the time coordinate and τ:

$$
\int_{\tau=0}^{\tau=20\pi}\left(\frac{\partial^2\theta}{\partial\xi^2}-2\frac{\partial\theta}{\partial\tau}\right)\cdot d\tau = 0
\tag{13}
$$

By imposing that the approximate equation satisfies the integral and applying a boundary conditions, we obtain:

$$
\begin{aligned}
&0.1014\,B_i\cos\left(0.8358-1.024\,B_i\right) \\
&-0.2078\cos\left(0.8358-1.024\,B_i\right) \\
&+\left(6.601\times10^{107719}+0.318 i\right)a''(\xi) \\
&-\left(1.5635\times10^{107724}-2i\right)a(\xi)+0.5795\,B_i^2 \\
&+4.682\,B_i-0.1014\,B_i\cos\left(1.024\,B_i+124.828\right) \\
&+0.2078\cos\left(1.024\,B_i+124.828\right)-3.302
\end{aligned}
\tag{14}
$$

$b.c.1)-\dfrac{\partial\theta^*}{\partial\xi}\bigg|_{0,\tau} = \hat{q}(\tau)-B_i\left(\theta-\theta_f\right)$

$$
\begin{aligned}
\Rightarrow\ &-a'(0)\mathrm{erf}\left(\tau^{1.5}\right)=\frac{1}{2}\left(1-\mathrm{sign}\left(\sin\left(\tau\right)\right)\right)\sin\left(\tau\right) \\
&-B_i\left((0.230-0.3528-B_i)\sqrt{\tau}\right. \\
&-(1-1.167\,B_i)(0.177-0.248\,B_i)\mathrm{erf}\left(\tau\right) \\
&+a(0)\mathrm{erfi}\left(\tau\right)+\left(0.186-0.156\,B_i\right)\sin\left(2.112-\tau\right)^3 \\
&+(0.207-0.101\,B_i)\sin\left(0.417-0.512\,B_i-\tau\right)^2 \\
&+(0.4437-0.2556\,B_i)\sin\left(0.5\tau\right)^2 \\
&+(0.235-0.1576\,B_i)\sin\left(\tau\right)^3 \\
&-(0.1587-0.1805\,B_i)\sin\left(1.5872+\tau\right)
\end{aligned}
\tag{15}
$$

$b.c.2)\quad \theta^*\left(\xi\to0,\tau\right)=0$

$$
\begin{aligned}
\Rightarrow\ &-\left(1-1.167\,B_i\right)\left(0.177-0.2483\,B_i\right)\mathrm{erf}\left(\tau\right) \\
&+\sqrt{\tau}\left(0.2307-0.3528\,B_i\right) \\
&+\left(0.1867-0.156\,B_i\right)\sin^3\left(2.112-\tau\right) \\
&+\left(0.235-0.157\,B_i\right)\sin^3\left(\tau\right) \\
&+\left(0.207-0.101\,B_i\right)\sin^2\left(-0.512\,B_i-\tau+0.417\right) \\
&+\left(0.443-0.255\,B_i\right)\sin^2\left(0.5\tau\right) \\
&-\left(0.158-0.1805\,B_i\right)\sin\left(\tau+1.587\right) \\
&+a(3)\mathrm{erfi}\left(\tau^{1.5}\right)=0
\end{aligned}
\tag{16}
$$

By solving the differential equation system (Eqs. (14)-(16)), the solution a(ξ) is obtained (Eq. (17)).

$$a(\xi) = -\frac{1}{\left(-3.32\times10^{200}B_i - 5.11\times10^{202}\right)\text{erfi}\left(\tau^{1.5}\right)}$$

$$\times 0.29\,e^{-153.9\xi}\text{erfi}\left(\tau^{1.5}\right)[0.53B_i^2\,e^{307.8\xi}\sin^3\left(2.11-\tau\right)$$

$$+82.21B_i\,e^{307.8\xi}\sin^3\left(2.11-\tau\right)-99.16\,e^{307.8\xi}\sin^3\left(2.11-\tau\right)$$

$$+B_i^3\,e^{307.8\xi}\text{erf}\left(\tau\right)+152.33B_i^2\,e^{307.8\xi}\text{erf}\left(\tau\right)$$

$$+1.21B_i^2\,e^{307.8\xi}\sqrt{\tau}+0.54B_i^2\,e^{307.8\xi}\sin^3\left(\tau\right)$$

$$+0.34B_i^2\,e^{307.8\xi}\sin^2\left(0.51B_i-\tau+0.41\right)$$

$$+0.88\,B_i^2\,e^{307.8\xi}\sin^2\left(0.5\tau\right)-0.62B_i^2\,e^{307.8\xi}\sin\left(\tau+1.58\right)$$

$$-241.29\,B_i\,e^{307.8\xi}\text{erf}\left(\tau\right)+186.58B_i\,e^{307.8\xi}\sqrt{\tau}$$

$$+82.89B_i\,e^{307.8\xi}\sin^3\left(\tau\right)$$

$$+53.14B_i\,e^{307.8\xi}\sin^2\left(0.51B_i-\tau+0.41\right)$$

$$+134.22B_i\,e^{307.8\xi}\sin^2\left(0.5\tau\right) \quad\quad (17)$$

$$-110.37e^{307.8\xi}\sin^2\left(0.51B_i-\tau+0.41\right)$$

$$-95.32B_i\,e^{307.8\xi}\sin\left(\tau+1.58\right)+94.27\,e^{307.8\xi}\text{erf}\left(\tau\right)$$

$$-122.53e^{307.8\xi}\sqrt{\tau}-124.81e^{307.8\xi}\sin^3\left(\tau\right)$$

$$-235.66e^{307.8\xi}\sin^2\left(0.5\tau\right)-5.19\times10^{-201}e^{307.8\xi}\sin\left(\tau\right)$$

$$+84.291e^{307.8\xi}\sin\left(\tau+1.587\right)$$

$$-5.198\times10^{-201}e^{307.8\xi}\sin\left(\tau\right)\text{sign}\left(\sin\left(\tau\right)\right)$$

$$+5.728\times10^{200}\sin\left(\tau\right)\,\text{sign}\left(\sin\left(\tau\right)\right)+5.728\times10^{200}\sin\left(\tau\right)]$$

$$-\left(1-1.167B_i\right)\left(0.177-0.248\,B_i\right)\text{erf}\left(\tau\right)$$

$$+\sqrt{\tau}\left(0.230-0.352\,B_i\right)+\left(0.186-0.156\,B_i\right)\sin^3\left(2.112-\tau\right)$$

$$+\left(0.235-0.157\,B_i\right)\sin^3\left(\tau\right)$$

$$+\left(0.207-0.1014\,B_i\right)\sin^2\left(0.512B_i-\tau+0.417\right)$$

$$+\left(0.443-0.255\,B_i\right)\sin^2\left(0.5\tau\right)$$

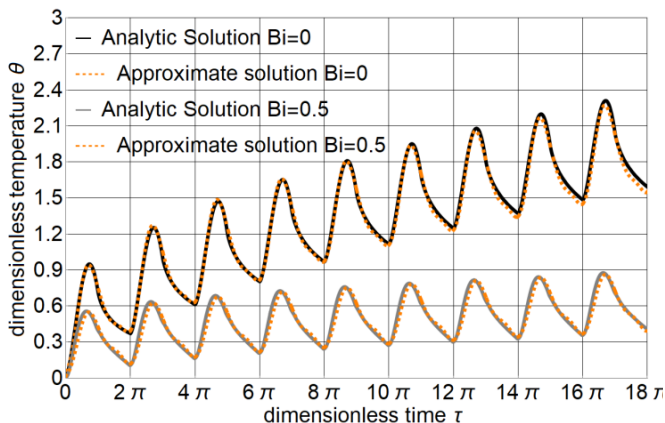$$-\left(0.158-0.180\,B_i\right)\sin\left(\tau+1.587\right)$$

Figure 5. The dimensionless surface temperature at $\xi = 0$ analytic vs approximate solution.

The complete solution is then derived using Eq. (12). It can be shown that the temperature profile resulting from the approximate solution (Eq. (12)) differs from that resulting from the corresponding analytical solution (Eq. (9)) by no more than 1.5% for Bi=0.5 and 1.2% for Bi=0 (Figure 5)

Temperature profiles as a function of revolution number were calculated using a dimensional formulation (Figure 6).
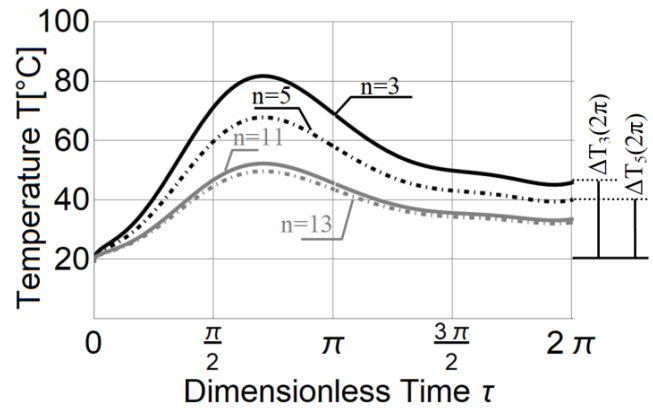

Figure 6. Surface temperature at $\xi = 0$ at different rpm values, $0 < \tau < 2\pi$.

The dimensional temperature profile was evaluated assuming $T_0 = 20$ °C, $\dot{q} = 40000$ W/m^2. The value of the heat flux was estimated by assimilating the emitter and the two-body tomato characterized by $\varepsilon = 1$ and uniform temperatures equal to 650°C and 60°C, respectively [13, 14, 18]. In the case of the tomato, it is considered an arbitrary thermal level corresponding to an intermediate value between the initial temperature and the final temperature assumed by it. The temperature level and, thus, the temperature fluctuation (ΔT) are reduced as n grows, as predicted, with sensitivity decreasing as n increases (Figure 5). In fact, for the same change in the number of revolutions, in this example from n=3 to n=5 rpm and from n=11 to n=13 rpm, at the lowest number of revolutions, temperature fluctuations are greatest. The temperature fluctuation (ΔT) for each lap was also evaluated for different rpm (Figure 7).
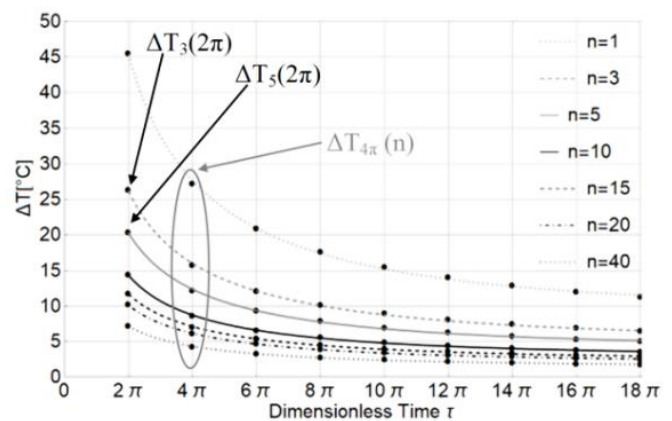

Figure 7. The Temperature Fluctuation as Function of τ at Different Values of rpm.

The exponential function is used to fit the data (Table 4):

$$\Delta T_n(\tau) = a\cdot\tau^b + c\cdot\tau \quad\quad (18)$$

Table 4. Coefficients of The Temperature Increase as Function of τ at Fixed n Value.

n	a	b	c
1	174.156	-0.735	0.0459
3	100.549	-0.735	0.0265
5	77.885	-0.735	0.0205
10	55.073	-0.735	0.0145
15	44.967	-0.735	0.0118
20	38.942	-0.735	0.0102
40	27.536	-0.735	0.0072

For regulation purposes, so, it is useful to evaluate, for each revolution, the temperature fluctuation $\Delta T_\tau(n)$ as a function of n (Figure 8, Table 5).
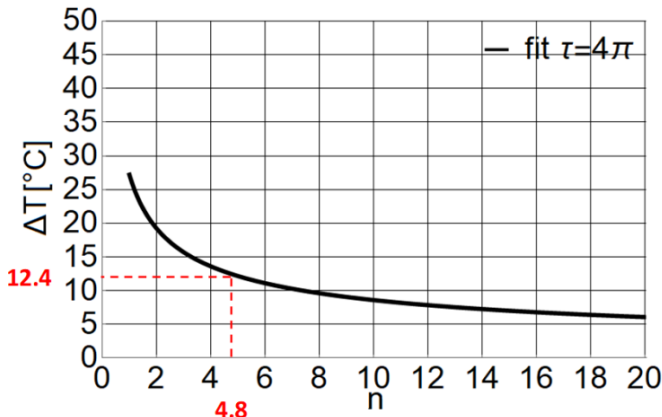

Figure 8. The temperature fluctuations $\Delta T_\tau(n)$ as function of n at τ=4π.

In order to fit the data, an exponential function is used likewise:

$$\Delta T_\tau(n) = A \cdot n^B + C \cdot n \tag{19}$$

Table 5. Coefficients of The Temperature Fluctuation as Function of n at Fixed τ Value.

τ	A	B	C
2π	45.494	-0.5	$4.651 \cdot 10^{-17}$
4π	27.206	-0.5	$3.334 \cdot 10^{-17}$
6π	20.876	-0.5	$4.450 \cdot 10^{-17}$
8π	17.599	-0.5	$2.031 \cdot 10^{-17}$
10π	15.505	-0.5	$5.520 \cdot 10^{-17}$
12π	14.017	-0.5	$5.007 \cdot 10^{-17}$
14π	12.890	-0.5	$9.302 \cdot 10^{-17}$
16π	11.998	-0.5	$4.924 \cdot 10^{-17}$
18π	11.269	-0.5	$1.054 \cdot 10^{-17}$

In this way, an estimate of the temperature fluctuation $\Delta T_\tau(n)$ for each period as the number of revolutions varies is obtained.

4. Logic Control

To realize successful peeling, surface temperatures are to be raised to values as high as 100°C in a very short warming up period, typically no more than 60 s [4, 8, 12]. By setting the revolution number to 10 rpm and the thermal flow value to 40000 W/m², the peeling process is completed in 51 s.

$$t_{end} = \tau_{end} \cdot t_{ref} = 17\pi(3/\pi) = 51 \text{ s} \tag{20}$$

As a consequence, after figuring out the number of revolutions necessary to get the best peeling quality, the dimensional temperature profile, obtained from the approximate solution with n = 10 rpm and Bi = 0, was used as a reference for the regulation system. Indeed, in the case of natural convection the value of Bi is very small, therefore for ease of calculation it was chosen equal to 0 [10, 11]. Particularizing the Eq. (12) in light of the considerations made, it is obtained:

$$T_{targ,\tau} = \theta^*(0,\tau) \cdot DT_{ref,n=10} + T_0 \tag{21}$$

with $DT_{ref,n=10} = \dot{q}_0 \cdot x_{ref}/k$. For regulation purposes, the error is evaluated at each revolution as follows:

$$err_\tau = T_{targ,\tau} - T_{sensor,\tau} \tag{22}$$

where $T_{sensor,\tau}$ is the surface temperature of the tomato detected by the sensor and $T_{targ,\tau}$ is the temperature corresponding to the reference temperature profile at the ith period (Eq. (21)). Thus, the temperature target fluctuations value ($\Delta T_{targ,\tau}$) necessary to reach the target temperature in the next period is obtained:

$$\Delta T_{targ,\tau+2\pi} = T_{targ,\tau+2\pi} - T_{sensor,\tau} \tag{23}$$

By particularizing Eq. (19) at time i+2π, the value of n to be used for regulation is obtained as shown:

$$\Delta T_{targ,i+2\pi} + err_i/2 = A_{(i+2\pi)} \cdot n^{B(i+2\pi)} + C_{(i+2\pi)} \cdot n \tag{24}$$

The equation that governs the control logic is represented by Eq. (24).

A straightforward illustration may be used to evaluate the method's efficacy. The value of emissivity is influenced by the geometric irregularity of the tomatoes and/or the presence of processing residues on the lamp's surface, which results in a reduction in the heat power transferred [10, 11, 19]. It is assumed that in the same working conditions (n = 10 rpm) the value of the radiative heat flux decreases to the value of $\dot{q}^* = 33000$ W/m². The decrease in the heat flow leads to the decrease in a reference temperature difference $(DT^*_{ref,n=10} = \dot{q}_0 \cdot x^*_{ref}/k)$, consequently the relative temperature profile $(T^*(0,\tau) = T_0 + \theta(0,\tau) \cdot DT^*_{ref})$ is lower than the reference one $(DT^*_{ref,n=10} < DT_{ref,n=10})$: heat flux reduces and hence the rate of temperature rises decreases. As a result of not enabling the regulation, the temperature profile $T^*(0,\tau)$ seen in Figure 9 is achieved. The peeling process, as shown, occurring at lower level temperature respect to reference profile, with a consequent lengthening of the process time. Ad-hoc regulation is implemented to keep the temperature profile similar to the reference one even if work conditions change. The number of revolution decreases when the temperature falls below the reference temperature, and vice versa.

Therefore, at the end of the first revolution (i = 2π), the error is evaluated (Eq. (22)):

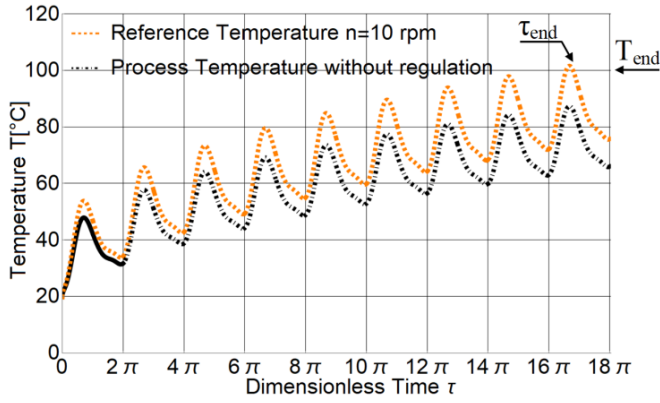$$err_{2\pi} = T_{targ,2\pi} - T_{sensor,2\pi} = 34.1 - 31.6 = 2.5 \tag{25}$$

Figure 9. Temperature profile without regulation.

The thermal response ($T_{sensor,\tau}$) is the result of simulated (through approximate solution) in the presence of a thermal power transferred by the lamps equal to $\dot{q}^*$ and a reference temperature difference $DT^*_{ref,n} = \frac{\dot{q}^* x_{ref.n}}{k}$, that depends to the number of revolutions used for the regulation. As the number of revolutions at the start of the thermal process is equal to 10 rpm, we get:

$$T_{sensor,2\pi} = T_{1°}(0,2\pi) = DT^*_{ref,n=10} \cdot \theta^*(0,2\pi) + T_0 \qquad (26)$$

with $T_{1°}(0,\tau)$ representing the temperature read by the pyrometer in the first period. Using Eq. (22), the target temperature is determined for the period 4π, and the temperature target fluctuation $\Delta T_{targ,i+2\pi}$ is then determined (Eq. (23)):

$$\Delta T_{targ,4\pi} = T_{targ,4\pi} - T_{sensor,2\tau} = 11.1°C \qquad (27)$$

Finally, by means of Eq. (24), particularized at time $\tau = i + 2\pi$, the correct value of n is obtained (Figure 8).

$$\Delta T_{targ,4\pi} + err_{2\pi}/2 = 27.206 \cdot n^{-0.5} + 4.651 \cdot 10^{-17} \cdot n \qquad (28)$$
$$\Rightarrow n = 4.8 \sim 5$$

A number of revolutions is chosen which, in the period between 2π and 4π, achieves a $\Delta T_{targ,4\pi}$ necessary to reach the target temperature at 4π, entered to consider the fact that the starting temperature is lower than in the reference case (+ err/2). By examining the second period to the Table 6 ($\tau = 2\pi : 4\pi$), we can observe that the sensor temperature is:

$$T_{2°}(0,4\pi) = DT^*_{ref,n=5} \theta^*(0,4\pi) + T_0 = 41.7 °C \qquad (29)$$

the target temperature is:

$$T_{targ,4\pi} = 42.7 °C \qquad (30)$$

It is observed how the error decreases from $err_{2\pi} = 2.5$ °C to $err_{4\pi} = 1$ °C. Proceeding in a similar manner for all periods, the temperature profile shown in Figure 10 is obtained.

It can be observed that, despite the working conditions differing from the preset ones, the regulation system manages to modify, by varying the rotation speed, the intensity of the heating, and consequently the temperature profile. In this way we have an effective method which allows us to have a standardized peeling process regardless of different working conditions.
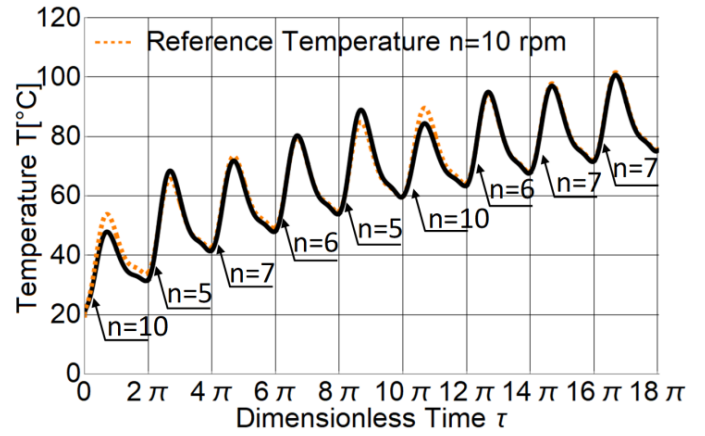

Figure 10. Temperature profile with regulation.

Table 6. Regulation Procedure: Evaluation of the Number of Revolutions.

p	1°	2°	3°	4°	5°	6°	7°	8°	9°
τ_{in}	0	2π	4π	6π	8π	10π	12π	14π	16π
τ_{end}	2π	4π	6π	8π	10π	12π	14π	16π	18π
n_p	10	5	7	6	5	10	6	7	7
Ω_p	$\pi/3$	$\pi/6$	$\frac{7\pi}{30}$	$\pi/5$	$\pi/6$	$\pi/3$	$\pi/5$	$\frac{7\pi}{30}$	$\frac{7\pi}{30}$
$t_{ref,p}$	$3/\pi$	$6/\pi$	$\frac{30}{7\pi}$	$5/\pi$	$6/\pi$	$3/\pi$	$5/\pi$	$\frac{30}{7\pi}$	$\frac{30}{7\pi}$
$x_{ref,p}$ [m]	5.2 10^{-4}	7.4 10^{-4}	6.2 10^{-4}	6.8 10^{-4}	7.4 10^{-4}	5.2 10^{-4}	6.8 10^{-4}	6.2 10^{-4}	6.2 10^{-4}
$\Delta T_{ref,p}$ [°C]	29.6	41.9	35.4	38.2	41.9	29.6	38.2	35.4	35.4
T_p [°C]	31.6	41.7	48.1	54.1	59.7	63.5	67.8	71.8	75.2
T_{targ} [°C]	34.1	42.7	49.3	54.9	59.8	64.2	68.3	72.1	75.7
$\Delta T_{targ,tend}$ [°C]	11.1	7.6	6.8	5.7	4.5	4.8	4.3	3.9	τ_{end}
err [°C]	2.5	1	1.2	0.8	0.1	0.7	0.5	0.3	

It can also be noted that the average temperature obtained from the regulated temperature profile Eq. (31) and that relating to the reference Eq. (32) case are generally the same, with only a very small error (Figure 11, Table 7)

$$\bar{T}_{reg} = \frac{\int_{\tau}^{\tau+2\pi} \theta^*(0,\tau)}{2\pi} DT^*_{ref,n_p} + T_0 \qquad (31)$$

with n_p indicating the number of revolutions selected for each period (Table 6).

$$\bar{T}_{targ} = \frac{\int_{\tau}^{\tau+2\pi} \theta^*(0,\tau)}{2\pi} DT_{ref,10} + T_0 \qquad (32)$$

Table 7. Average Temperature in the Period.

τ_{ini}	τ_{end}	$\bar{T}_{targ}$	$\bar{T}_{reg}$
0	2π	39.8	36.3
2π	4π	50.7	51.0
4π	6π	58.2	56.9
6π	8π	64.2	64.0
8π	10π	69.4	70.9
10π	12π	74.1	71.7
12π	14π	78.3	78.4
14π	16π	82.3	81.7
16π	18π	85.9	85.4
	mean	67	66.3

The maximum error is obviously detected at the end of the first period where the regulation system has not yet intervened.
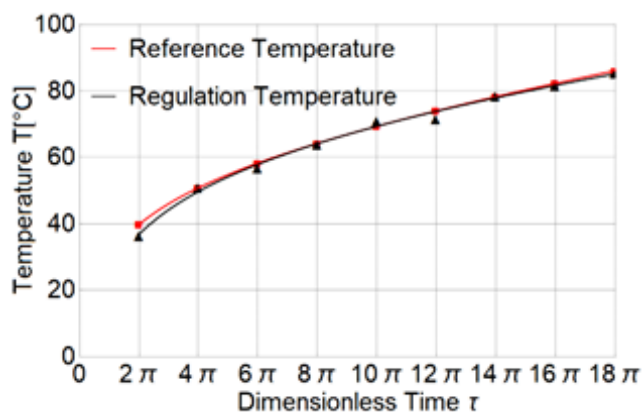

Figure 11. Average temperature.

Thus, even though the set-up conditions are different , a peeling process has been got that's entirely similar to the individual thought-out optimum, both in thermal conditions and in terms of quality. We can recap it as follows (Figure 12):
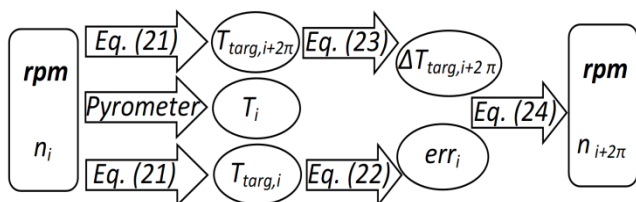

Figure 12. Regulation procedure.

- o Known the optimal value of n, the peeling process starts.
- o At the end of the i period, through Eq. (21), we extract the T_{targ}, at period i and at period $i+2\pi$, and through the pyrometer the temperature of tomato.
- o Eq. (23) allows us to calculate the temperature jump required to reach the target temperature at the next period, while Eq. (22) the error.
- o Using Eq. (24), the number of revolutions for the following period is obtained

5. Conclusion

After having carried out a preliminary study and having obtained the value of the rotation speed, and therefore of the temperature profile, which makes it possible to obtain a peeling of excellent quality, at the chosen set-up (distance and power of the IR lamp, average diameter of the tomatoes, etc.), it is important to put in a logic of control which allows us to obtain a conforming to that sought when the set-up conditions vary. Any cause that takes us away from pre-established conditions, for example a diameter of the tomato lower than that tested in the preliminary study, can be assimilated to a variation in thermal power exchanged between the lamp IR and tomato. In particular, the surface temperature of the tomato has a lower profile than the reference one if the thermal power is lower, vice versa in the opposite case. Therefore, to obtain the same temperature profile for the peeling process, a control logic has been put in place which allows the thermal power between the IR lamp and the tomato to be varied by adjusting the number of revolutions. Through the study of the analytical model and the approximate solution, an estimate of the amplitude of temperature fluctuations $\Delta T(n)$ for each period as the number of revolutions varies was obtained. Consequently, the Eq. (24) is used to determine the value of the number of revolutions for the following period after evaluating the temperature error between the sensor temperature and the target temperature (obtained from the approximated solution) at each period and the temperature jump required to reach the target temperature at the next period. This results in a standardized peeling process in terms of process time, temperature and quality.

Nomenclature

ρ	Mass density	Kg m^{-3}
c_p	Specific heat	J kg^{-1} K^{-1}
α	Thermal diffusivity	m s^{-2}
k	Thermal conductivity	W m^{-1}K^{-1}
Ω	Period	s
n	Number of revolution	rpm
x_{volume}	Volume fraction	/
x_{mass}	Mass fraction	/
τ	Dimensionless temperature	/
θ	Dimensionless time	/
ξ	Dimensionless x	/
Bi	Biot number	/
ε	Emissivity	/

References:

[1] C. Rock, W. Yang, R. Goodrich-Schneider, H. Feng, "Conventional and Alternative Methods for Tomato Peeling", *Food Engineering Reviews* , 4(1), 1–15, 2012.

[2] J. Shi, M. Le Maguer, "Lycopene in tomatoes: chemical and physical properties affected by food processing", *Critical Reviews in Food Science and Nutrition* , 40(1), 1-42, 2000.

[3] E. Garcia, D. M. Barrett, "Peelability and yield of processing tomatoes by steam or lye", *Journal of Food Processing and Preservation,* 30(1), 3-14, 2006.

[4] Z. Pan, X. Li, R. Khir, H. M. El-Mashad, G. G. Atungulu, T. H. McHugh., M. Delwiche, "A pilot scale electrical infrared dry-peeling system for tomatoes: Design and performance evaluation", *Biosystems engineering,* 137, 1-8, 2015.

[5] S. Vidyarthi, X. Li, Z. Pan, "Peeling of tomatoes using infrared heating technology", *Tomato Chemistry, Industrial Processing and Product Development, 180-200,* 2019.

[6] X. Li, Z. Pan, G. G. Atungulu, X. Zheng, D. Wood, M. Delwiche, T. H. McHugh, "Peeling of tomatoes using novel infrared radiation heating technology", *Innovative Food Science & Emerging Technologies*, 21, 123-130 , 2014.

[7] X. Li, Z. Pan, G. G. Atungulu, D. Wood , T. H. McHugh, "Peeling mechanism of tomato under infrared heating: Peel loosening and cracking", *Journal of Food Engineeri*ng , 128, 79–87, 2014.

[8] X. Li, Z. Pan, "Dry peeling of tomato by infrared radiative heating: Part I. Model Development", *Food Bioprocess Technol, 7, 1996-2004,* 2014.

[9] X. Li, Z. Pan, "Dry peeling of tomato by infrared radiative heating: Part II. Model Validation and Sensitivity Analysis", *Food and Bioprocess Technol* 7, 2005-2013, 2014.

[10] G. Cuccurullo, L. Giordano; "Temperature field for radiative tomato peeling"; *J. Phys.: Conf. Ser.*, 796, 1, 2017.

[11] G. Cuccurullo, L. Giordano, A. Metallo, *"*Analytical solutions for tomato peeling with combined heat flux and convective boundary conditions", *J. Phys.: Conf. Ser.*, 923, 2017.

[12] Z. Pan, X. Li, G. Bingol, T. H. McHugh, G. G. Atungulu, "Development of infrared radiation heating method for sustainable tomato peeling", *Applied Engineering in Agriculture*, 25(6), 935- 941, 2009.

[13] D. C. Hamilton, W. R. Morgan . *Radiant-interchange configuration factors*, NASA TN 2836, 1952.

[14] H. C. Hottel. *Radiant heat transmission*, William H. McAdams (ed.), Heat Transmission, 3rd ed., McGraw-Hill Book Co., New York., 55-125, 1954.

[15] Z. Pan, G.G. Atungulu, *Infrared heating for food and agricultural processing*. CRC Press, 2010.

[16] S. K. Vidyarthi, H. M. El Mashad, R. Khir, S. K. Upadhyaya, S. K .Singh, R. Zhang, R. Tiwari, Z. Pan, "A mathematical model of heat transfer during tomato peeling using selected electric infrared emitters", *Biosystems Engineering,* 186, 106-117, 2019.

[17] Y. H. Choi, "Effects of temperature and composition on the thermal properties of foods", *Korean Journal of Food Science and Technology,* 18(5), 357-363, 1986.

[18] S. K. Vidyarthi. H. M. El Mashad, R. Khir, R. Zhang, R. Tiwari, Z. Pan, "Evaluation of selected electric infrared emitters for tomato peeling", *Biosystems Engineering* 184, 90-100, 2019.

[19] X. Li, Z. Pan, G. G. Atungulu, X. Zheng, D. Wood, M. Delwiche, T. H. McHugh, "Peeling of tomatoes using novel infrared radiation", *Innovative Food Science & Emerging Technologies,* 21, 123-130, 2014.

[20] G. Cuccurullo, L. Giordano; "Simplified numerical modelling of infrared radiation effects in tomato dry peeling, *J. Phys. Conf. Ser.,* 1224(1), 2019.

[21] K. Krishnamurthy, H. K. Khurana, J. Soojin, J. Irudayaraj, A. Demirci, "Infrared heating in food processing, an overview*", Comprehensive reviews in food science and food safety,* 7(1), 2-13, 2008.

[22] Li, X. (2012). *A study of infrared heating technology for tomato peeling: process characterization and modeling* (PhD. Dissertation). University of California, Davis.

[23] Prakash, B. (2012). *Mathematical modeling of moisture movement within a rice kernel during convective and infrared drying* (Ph.D. Dissertation), University of California, Davis.

[24] H. Togrul, "Simple modeling of infrared drying of fresh apple slices", *Journal of Food Engineering*, 71(3), 311-323, 2005.

[25] H. J. Hellebrand, H. Beuche, M. Linke, "Determination of thermal emissivity and surface temperature distribution of horticultural products", in: *Sixth international symposium on fruit, nut and vegetable production engineering*, Potsdam, Germany, pp. 1497-1504, 2001.

[26] X. Li, Z. Pan, H. Bingol, T. H. McHugh, "Feasibility study of using infrared radiation heating as a sustainable tomato peeling method", *2009 Reno, Nevada, June 21-June 24, 2009*. American Society of Agricultural and Biological Engineers, 2009.

[27] R. P. Singh,, D. R. Heldman, *Introduction to Food Engineering: Edition 4*, Academic Press Inc., London, 2010.